THE ASTROPHYSICAL JOURNAL, 473:7–14, 1996 December 10

THE ANGULAR TWO-POINT CORRELATION FUNCTION FOR THE FIRST RADIO SURVEY

CATHERINE M. CRESS,[1] DAVID J. HELFAND,[1] ROBERT H. BECKER,[2,3]
MICHAEL D. GREGG,[3] AND RICHARD L. WHITE[4]
Received 1996 January 25; accepted 1996 July 2

ABSTRACT

The FIRST (Faint Images of the Radio Sky at Twenty centimeters) survey now covers 1550 deg^2 of sky, where $07^h16 \lesssim \alpha \lesssim 17^h40$ and $28^\circ.3 \lesssim \delta \lesssim 42^\circ$. This yields a catalog of 138,665 sources above the survey threshold of 1 mJy, about one-third of which are in double-lobed and multicomponent sources. We have used these data to obtain the first high-significance measurement of the two-point angular correlation for a deep radio sample. We find that the correlation function between $0^\circ.02$ and 2° is well fitted by a power law of the form $A\theta^\gamma$, where $A \approx 3 \times 10^{-3}$ and $\gamma \approx -1.1$. On small scales ($\theta < 0^\circ.2$), double and multicomponent sources are shown to have a larger clustering amplitude than that of the whole sample. Sources with flux densities below 2 mJy are found to have a shallower slope than that obtained for the whole sample, consistent with there being a significant contribution from starbursting galaxies at these faint fluxes. The cross-correlation of radio sources and Abell clusters is determined. A preliminary approach to inferring spatial information is outlined.

Subject heading: cosmology: theory — galaxies: clusters: general — galaxies: statistics — large-scale structure of universe — surveys

1. INTRODUCTION

Correlation-function analysis has become the standard way of quantifying the clustering of different populations of astronomical sources. Much of the interest in this type of analysis stems from its potential to constrain the spectrum of density fluctuations present in the early universe, and thus to constrain the physics of the early universe. While it is the spatial correlation function that is directly related to the power spectrum, the *angular* correlation function of galaxies in optical surveys has been used to infer the spatial correlation function when redshift information was not available. These inferred values have later been shown to agree with measured values of the spatial correlation (cf. Groth & Peebles 1977 and Davis & Peebles 1983). In addition, in all but the deepest optical surveys, the amplitude of the angular galaxy-galaxy correlation function [A, in $w(\theta) = A\theta^\gamma$, $\gamma \approx -0.8$] is found to scale with the depth of the survey as described in Peebles (1980). Very faint galaxies might have a slightly flatter slope, but the fact that A generally scales in this well-understood way supports the use of the angular correlation function as a probe of large-scale structure (and thus a probe of the density fluctuation spectrum in the early universe).

Optical surveys covering large regions of sky have provided much information on large-scale structure out to a redshift of $z \approx 0.1$. In addition, "pencil-beam" surveys have given some information on structure at redshifts beyond this. Radio surveys, however, generally sample much larger volumes of space than any optical surveys and so have the potential to provide information on much larger physical scales. It has been thought that the broad luminosity function of radio sources, however, might wash out any spatial correlations in the angular projection. This idea was supported by the work of Webster (1976), who determined the angular power spectrum of the 4C and GB radio surveys, and by the work of Masson (1979), who determined the angular correlation function for the 6C catalog. The catalogs they used contained only the very brightest radio sources, and neither found any evidence for clustering. More recently, however, Peacock & Nicholson (1991) have shown that bright radio sources (flux density, $S > 2$ Jy) in a narrow redshift band ($0.01 < z < 0.1$) are spatially correlated, the sources showing the power-law behavior $\xi = (r/11\ h^{-1}\ \mathrm{Mpc})^{-1.8}$. Shaver & Pierre (1989) also found some evidence of clustering toward the supergalactic plane for radio sources with $z < 0.02$. In addition, marginal detections of a nonzero angular correlation function have been found for sources with $S > 35$ mJy in the Green Bank 4.85 GHz survey (Kooiman, Burns, & Klypin 1995; Sicotte 1995), suggesting that spatial correlations will indeed show up in the angular projection if a survey goes to faint enough fluxes.

The FIRST (Faint Images of the Radio Sky at Twenty centimeters) survey is 50 times more sensitive than any previous radio survey, and thus provides an excellent opportunity to investigate the angular correlation function of faint sources and to explore the possibility of inferring spatial information from this measurement. In § 2, we describe the catalog of ~138,000 sources used in the study. We then outline the methods we have adopted to compute the angular correlation function and the errors thereon (§ 3). Section 4 presents the results for the catalog as a whole, as well as for various subsamples; in § 5, we compare our results with previous work and outline a preliminary approach for obtaining information on the spatial correlation of radio sources. In § 6, we summarize our conclusions.

2. THE CATALOG

The goal of FIRST is to survey, at 1.4 GHz, the 10,000 deg^2 at the north Galactic cap scheduled for inclusion in the

[1] Department of Astronomy, Columbia University, 538 West 120th Street, New York, NY 10027.
[2] Department of Physics, University of California, Davis, CA 95616.
[3] Institute of Geophysics and Planetary Physics, Lawrence Livermore National Laboratory, Livermore, CA 94450.
[4] Space Telescope Science Institute, 3700 San Martin Drive, Baltimore, MD 21218.

Sloan Digital Sky Survey. The 5 σ source detection threshold is $\sim$1 mJy. With a positional accuracy better than 1″ and $\sim$100 sources per square degree, confusion is not a problem. By 1995 October, $\sim$15% of the survey had been completed, and a catalog containing 138,665 sources with $07^h16 < \alpha < 17^h36$ and $28.^\circ3 < \delta < 42^\circ$ was released (White et al. 1996, hereafter WBGH). Approximately 30% of these sources are within 0.′02 of another source and so, for the purposes of the correlation-function analysis, are considered part of double-lobed or multicomponent systems.

The details of the data analysis, map production, and catalog generation are given in Becker, White, & Helfand (1995, hereafter BWH) and in WBGH. In brief, images are produced at each point in a grid designed to provide an efficient and uniform tiling of the sky. These images are truncated at an off-axis angle of 23.′5, weighted and summed to yield a set of co-added maps containing 1550 × 1150 1.″8 pixels. The rms noise at each point in the co-added maps is calculated from the weighted sum of the measured noise values in each of the images that contribute to that point. Sources with flux densities greater than 5 times the rms noise and a peak flux density $\geq$1.0 mJy are included in the preliminary catalog, which is then screened for spurious sources using the algorithms discussed in BWH. Of the 138,665 sources, 4813 were flagged as possible sidelobes. Our analysis indicates that less than 10% of the flagged sources are real sources, while less than 1% of unflagged sources are spurious (see below).

BWH estimate the catalog to be 95% complete to 2 mJy and 80% complete to 1 mJy. This estimate was inferred from comparison with a deep VLA survey containing only 49 sources, but one obtains similar predictions by taking the sources detected in the Westerbork-Leiden-Berkeley Deep Survey and accounting for the effects of the CLEAN bias, resolution effects, and the adopted peak flux density threshold. It appears that only the most extended objects are missing from the catalog. Completeness studies are discussed further in BWH and in WBGH.

A coverage map has been calculated for the survey, providing effective sensitivity estimates with $\sim$4′ resolution. A region is considered to be covered if the sensitivity at all points in the area is greater than 0.75 times that at the center of the pointing. This map has been used to establish the large-scale uniformity of the survey. On scales smaller than the co-added image size (34.′5 × 46.′5), BWH claim that the variation in noise level is less than 15%, with the sensitivity pattern repeated from one field to the next.

3. DETERMINING THE CORRELATION FUNCTION

The two-point angular autocorrelation function is defined by the joint probability δP of finding two sources in each of the elements of solid angle $\delta\Omega_1$ and $\delta\Omega_2$ separated by angle θ:

$$\delta P = N^2[1 + w(\theta)]\delta\Omega_1\delta\Omega_2 , \quad (1)$$

where N is the mean surface density. Many derivations for estimators of $w(\theta)$ have been given before (see, for example, Peebles 1980). For those unfamiliar with the field, we outline a basic derivation given by Sicotte (1995).

It follows from the definition that, for a catalog of n data points covering a solid angle Ω, the mean number of sources at a distance $\theta \pm \Delta\theta$ from a randomly picked data point is $(n-1)[1 + w(\theta)]\langle\delta\Omega\rangle/\Omega$, where $\langle\delta\Omega\rangle$ is the mean solid angle about a randomly chosen data point. The total number of pairs with separations in the interval $\theta \pm \Delta\theta$ is then given by $DD(\theta) = (n/2)(n-1)[1 + w(\theta)]\langle\delta\Omega\rangle/\Omega$. $DD(\theta)$ can be measured directly from the catalog and, when combined with an estimate of $\langle\delta\Omega\rangle/\Omega$, can give an estimate of $w(\theta)$. For an all-sky catalog, $\delta\Omega = 2\pi \sin(\theta)\Delta\theta$ and $\Omega = 4\pi$. For surveys with complicated geometries, it is more practical to calculate $\langle\delta\Omega\rangle/\Omega$ by using a field of randomly distributed points that cover the same area as the survey. Assuming there are the same number of random points as there are data points, the number of pairs of random points with separations between $\theta \pm \Delta\theta$ is given by $RR(\theta) = (n/2)(n-1)\langle\delta\Omega_r\rangle/\Omega$. One can clearly measure this quantity and obtain a value for $\langle\delta\Omega_r\rangle/\Omega$ that is approximately equal to $\langle\delta\Omega\rangle/\Omega$. A simple estimator of $w(\theta)$ is thus given by $DD/RR - 1$. Strictly speaking, one needs to have more random points than data points so that the $w(\theta)$ estimate is not limited by statistical errors in the random points. An improvement on this estimate of $\langle\delta\Omega\rangle/\Omega$ can be obtained by using the quantity $DR(\theta)$: the number of pairs of points separated by angle θ, where one point is taken from the data field and one is from the random field. Using DR instead of RR enables one to measure the mean solid angle around data points ($\langle\delta\Omega\rangle/\Omega$) as opposed to the mean solid angle around random points ($\langle\delta\Omega_r\rangle/\Omega$).

Sicotte (1995) gives a detailed comparison of the various estimators of $w(\theta)$. We have chosen to quote results using the standard (S) estimator [$w(\theta) = 2DD/DR - 1$] as well as the estimator suggested by Landy & Szalay (1993, hereafter LS) [$w(\theta) = (DD - DR + RR)/RR$]. The LS estimator has been shown to have smaller uncertainties on larger scales, and Sicotte claims it will remove the effects of large-scale fluctuations in density for estimates of $w(\theta)$ at small θ. The method introduced by Hamilton (1993) [$w(\theta) = 4(DD \times RR)/(DR \times DR) - 1$)] gives results very similar to the LS estimator.

To determine the uncertainties associated with each estimate, a "bootstrap" analysis of the errors was performed. This method of estimating uncertainties is described in detail in Ling, Frenk, & Barrow (1986) and in Fisher et al. (1994). A set of "bootstrap" catalogs, each the same size as the data catalog, is generated using the following procedure. A source is picked at random from the data catalog and inserted into the first bootstrap catalog. Random sources from the data catalog continue to be included in the bootstrap catalog, until it has the same number of sources as the data catalog. Some of the sources in the original data set will appear more than once in the bootstrap catalog, some will not appear at all. A set of these bootstrap catalogs can then be generated, and the correlation function can be calculated for each one. The result is that, at each θ, we produce a set of normally distributed estimates of the correlation function. The variance around the mean can then be used as an estimate of the uncertainty in the measurement of w at each θ. This process established that both the S estimator and the LS estimator of $w(\theta)$ had similar uncertainties associated with them out to about 10°. The Poissonian estimate of the uncertainties given by $\Delta w = [(w(\theta) + 1)]/[DD(\theta)]^{0.5}$ is less than the bootstrap estimate by a factor of 2 on small scales ($\sim$0.′05) and by more than an order of magnitude on larger scales ($\sim$5°).

As explained above, the random field measurements RR and DR correct for the "edge effects," that is, they estimate the mean solid angle about points in the area of the survey for a given θ. Therefore, the random field should contain all

the biases that the data field contains. We consider the following:

1. In the correlation analysis, we have used a catalog in which all sources within 0.°02 of each other are considered a single source. This constraint is reproduced in the random fields.

2. The coverage of the data is reproduced in the random fields by using the 2060 × 299 pixel coverage map, where each pixel represents a 4.′5 × 3′ (R.A. × decl.) area. Random points are generated in any region where there is data coverage. The flux density threshold for detection of a source depends on the local rms noise, which varies slightly across the survey area. To check whether any systematic variations in sensitivity could affect the correlation-function estimate, we used the coverage map to generate a random field that also "missed" sources in noisy areas, even though they had a flux density of $S > 1$ mJy. Random sources were assigned a random flux density according to the Windhorst et al. (1985) log N–log S curve. If the source flux density was below 5 times the rms noise given in the coverage map, then it was discarded. The results of this are noted in § 4.1

3. The presence of sidelobe contamination could also be included in the random fields. Instead, we decided to use the correlation function to obtain an independent estimate of the sidelobe contamination.

In addition to the angular autocorrelation function for the catalog as a whole and various source subsamples, we have determined the angular cross-correlation function for the radio sources and Abell clusters. We use the estimator $w_{\rm cross}(\theta) = Dd/Rd - 1$, where Dd is the number of radio sources separated by $\theta°$ from an Abell cluster center and Rd is the number of random field points $\theta°$ from an Abell cluster center.

4. RESULTS

The correlation function fit parameters for various subsamples are given in Table 1.

4.1. *The Whole Sample*

A catalog of 109,873 sources was generated by collapsing all sources that are within 0.°02 of each other to a single source, since the majority of such cases represent multiple components of a single host object (e.g., double radio lobes). This sample contains predominantly radio-loud, giant elliptical galaxies, quasars, and starbursting galaxies (Windhorst et al. 1985). (Becker et al. 1996 have shown that stars make up less than 0.1% of the sources.) The correlation function of such a mixed sample is difficult to interpret, but it serves as a starting point for investigating specific subsamples. The correlation function for all sources in the catalog with $07^{\rm h}16 < \alpha < 17^{\rm h}36$ and $28.°3 < \delta < 42°$ was determined by using both the LS estimator $[w(\theta) = (DD - DR + RR)/RR]$ and the S estimator $[w(\theta) = 2DD/DR - 1]$. The RR and DR used are the average of 10 random field generations. The results for the S estimate are displayed in Figure 1. The error bars shown are random errors determined by using the bootstrap algorithm described above.

To determine the parameters of a power-law fit of the form $A\theta^{\gamma}$, a straight line was fitted to the log-log plots (for collapsed sources) out to 2° using standard χ^2 minimization. This yields $A = (3.7 \pm 0.3) \times 10^{-3}$ and $\gamma = -1.06 \pm 0.03$ for the S estimator, and $A = (2.0 \pm 0.3) \times 10^{-3}$ and $\gamma = -1.26 \pm 0.04$ for the LS estimator. For the LS estimate to be a better estimate than the S estimate, one requires many more random points in a field than data points. With about 10^5 data points, the number of random points is severely limited by computer time. The S estimate is thus probably more reliable.

Figure 1 also shows correlation-function estimates obtained when sources separated by less then 0.°02 are not collapsed. As is expected, one sees a large increase in the correlation function on small scales resulting from single sources being counted as two or more sources. On the scales of our fit, however, there is little difference between the two, indicating that the small percentage of unassociated sources that have been merged do not affect the correlation function significantly.

There are two problems with fitting a straight line to determine power-law parameters. The first is that normal errors in the original data do not translate to normal errors in the log-log plot as required for χ^2 fitting. To check the effects of this, we used the Levenberg-Marquardt technique to fit a function of the form $A\theta^{\gamma}$ to the original (linear-linear) data. It was found that the slopes and amplitudes agreed to well within 1 σ with the straight-line fits; we thus consider the straight-line fits to be adequate. The second problem is that the correlation-function estimates at different θ are not independent. In calculating the correlation function for a sample of optical galaxies, Bernstein (1994) used principal component analysis to obtain linearly independent combinations of their measurements, which could then be used in a χ^2 fit. It did not appear to affect their estimates of the parameters significantly (although the effect on error estimates can be more substantial).

As a test of our procedures, random fields were generated and analyzed as though they were data fields. It was found that the $w(\theta)$ were consistent with zero.

TABLE 1

CORRELATION ANALYSIS RESULTS

Sample	Source Type	Source Number	Amplitude ($\times 10^{-3}$)	Power (γ)
All sources	Mixed	109,873	3.7 ± 0.3	-1.06 ± 0.03
Double + multi.....	FR I and II	17,773	3.8 ± 0.5*	-1.39 ± 0.4
Single	UFR, SB, and C	92,057	5.2 ± 0.4	-0.84 ± 0.05
Single ($S > 3$ mJy).....	UFR, C, and SB	33,800	1.9 ± 0.4	-1.10 ± 0.07
Single ($S < 2$ mJy).....	SB, UFR, and C	45,312	8.2 ± 1.0	-0.84 ± 0.05
All × Abell	Mixed × clusters	109,873 × 382	13.5 ± 4.8	-1.07 ± 0.2

NOTES.—Fitted parameters for various subsamples of data. Values are obtained from the ($DD/DR - 1$) method of estimation. Fitting is done out to 2°, except for the one labeled with an asterisk, which is fitted to 0.°2. C refers to "compact" sources, SB refers to starburst galaxies, and FR refers to the Fanaroff-Riley classification (U stands for unresolved).

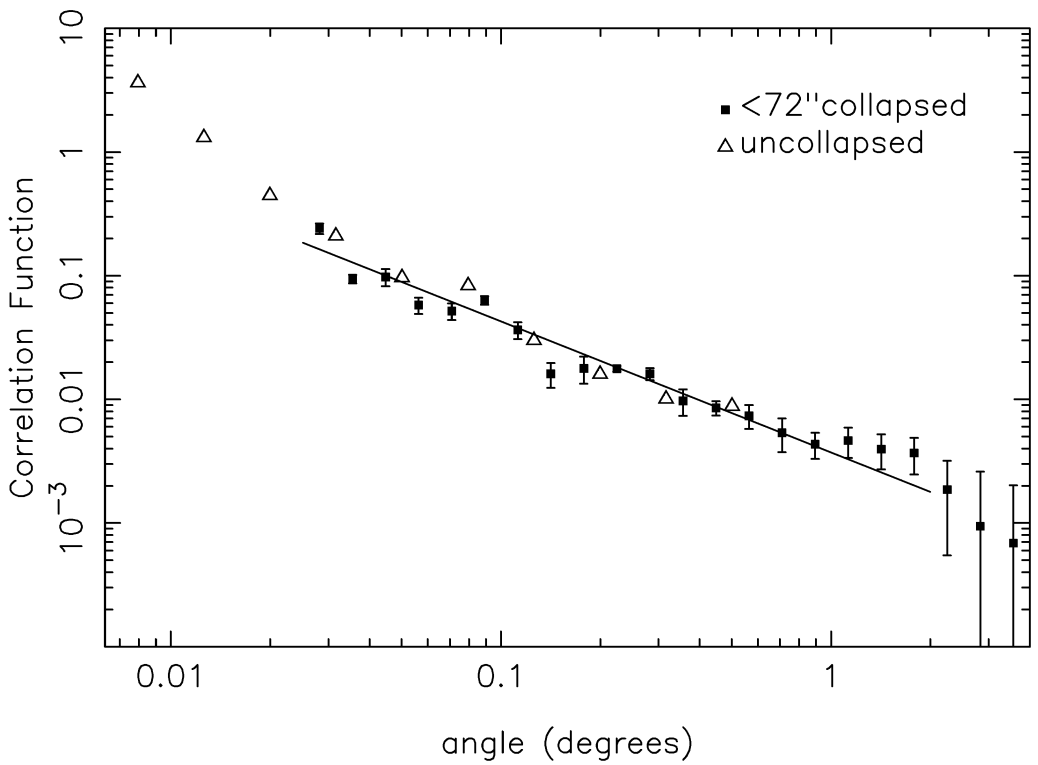

FIG. 1.—The filled squares show the autocorrelation function [$w(\theta) = 2DD/DR - 1$] calculated for the whole sample (109,873 sources, where sources separated by less than 0.°02 have been collapsed to a single source). The open triangles show the correlation function obtained when sources are not collapsed. Error bars are obtained using the bootstrapping technique described in § 3.

Some systematic differences in the uniformity of the survey are evident in the correlation functions. The result for the sample that *includes* the sources flagged as sidelobes (not plotted) shows a sudden increase in $w(\theta)$ at 6′. When flagged sources are removed (as in the figures shown here), the bump decreases in size but is still noticeable, particularly in the result for double and multicomponent sources. Six arcminutes is the distance of the first sidelobe in unCLEANed VLA B-configuration images, so the "bump" is a clear indicator that not all sidelobes have been removed. The situation is worse for double and multicomponent sources because the sidelobes from such extended sources are harder to remove in the standard CLEANing process. To further investigate the effect of sidelobes on the correlation function, varying fractions of spurious sources were added at 6′ from real data points. Results indicate that the distortion in the correlation function is fairly well localized to 6′ and that about ∼1% of all the (collapsed) sources remaining in the catalog are sidelobes. Efforts to improve the efficiency of our sidelobe flagging algorithms are in progress.

The first point in the correlation function for the whole sample appears high. This could be attributed to the presence of double-lobed galaxies that have separations larger than 0.°02, the adopted radius within which we call all detected components a single radio source. There is also a significant dip in $w(\theta)$ at ∼10′. This could be related to the CLEANing procedure or to the systematic nonuniformity in sensitivity that is repeated from one co-added map to another. To investigate this further, we included the sensitivity fluctuations given in the coverage map in the random field (as described in § 3). This did result in a smoother estimate at 10′; in addition, the first point in the correlation function was also slightly lower. Fitting a straight line to the log-log data, which included the sensitivity fluctuations, returned parameters that were within 1 σ of those that did not include sensitivity fluctuations (given above).

Cross-correlating the whole sample with Abell clusters results in a power-law fit with an amplitude ∼3.6 times that of the autocorrelation (see Fig. 2). In the future, we will investigate the possibility of combining this information with spatial information for clusters in order to infer spatial information for radio sources.

4.2. *Double and Multicomponent Sources*

A catalog of double and multicomponent sources (resolved, extended sources) was generated by considering any sources separated by less than 0.°02 to be part of a single multicomponent source. Results for this subsample of 17,773 sources using the S estimator are shown for $\theta < 0.°2$ in Figure 3. Force fitting a line with the same slope as the whole sample yields an amplitude of $A = 9.5 \times 10^{-3}$, a factor of 2.7 times larger than that for the sample as a whole. Fitting a straight line on these small scales yields $A = (3.8 \pm 0.5) \times 10^{-3}$ and $\gamma = -1.4 \pm 0.4$. On larger scales, many of the error bars extend below zero, so we fitted the linear-linear data using the Levenberg-Marquardt technique. This yields $A = 1.65 \times 10^{-3}$ and $\gamma = -1.36$ out to 1°, but this does not fit the points on small scales very well.

Traditionally, those radio sources that can be resolved into components have been classified into one of two groups (Fanaroff & Riley 1974): FR II sources are the more luminous [$\log P(\mathrm{W\ Hz^{-1}}) \gtrsim 25$] "classical doubles," while FR I sources have distorted lobe structures and generally have lower luminosities. FR II sources are known to prefer

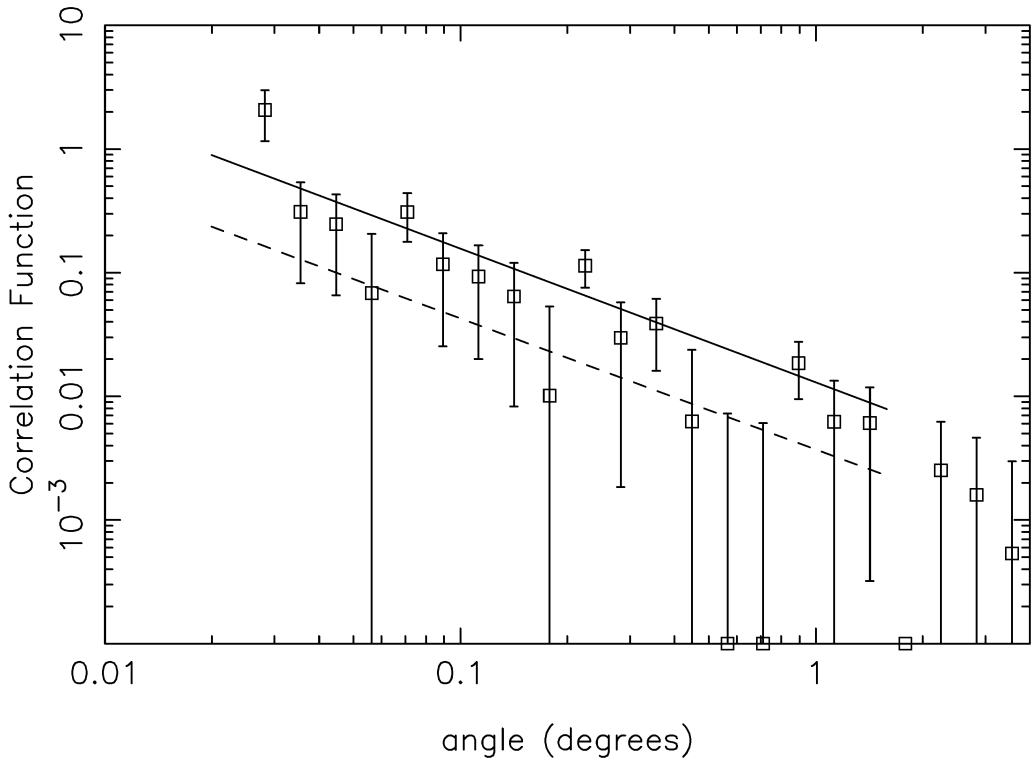

FIG. 2.—The cross-correlation function of the whole sample of radio sources with Abell clusters, using the $Dd/Rd - 1$ estimator. The solid line shows the best fit to the cross-correlation results, while the dotted line shows the best fit to the autocorrelation of the radio sources (S) estimator. Error bars show Poissonian errors [$\Delta w = (w + 1)/DD^{0.5}$].

lower density environments than FR I sources at low z, but Hill & Lilly (1991) have shown that, at $z \sim 0.5$, FR II sources also exist in higher density regions. In an attempt to estimate the correlation for FR II and FR I sources separately, the catalog of multiple sources was split into a catalog containing double sources only and a catalog containing sources with more than two components. The small number of points resulted in a large amount of scatter, particularly

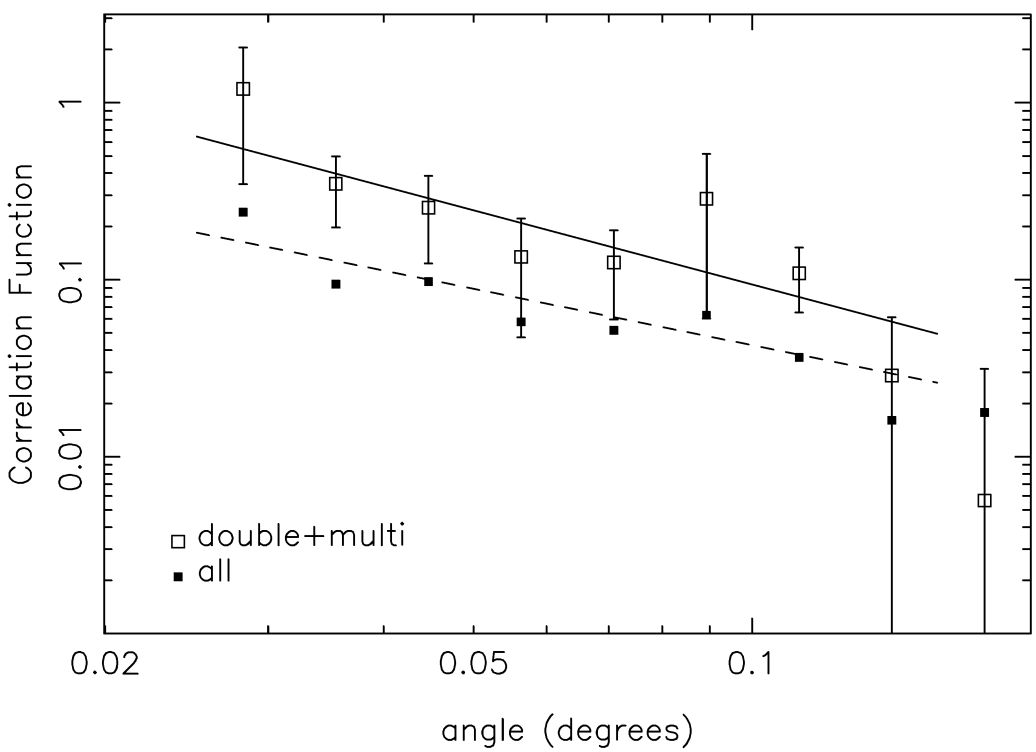

FIG. 3.—The open squares show the autocorrelation function for the double and multicomponent systems using the S estimator, with the solid line showing the best fit to the points. The filled squares and dashed line are the same as those shown in Fig. 1.

on larger scales, but on small scales ($\theta < 0.^\circ 2$), it appeared that the multicomponent sources (predominantly FR I sources) were, as expected, more clustered than the double sources (FR II sources) by about a factor of 2–3.

Using the preliminary catalog of sources with $28^\circ < \delta < 31^\circ$ that was available at the beginning of 1995, a catalog of double sources was generated using stricter selection criteria than those used here. In addition to the requirement that there be two (and only two) sources separated by less than $0.^\circ 02$, the fluxes of the sources were required to be within a factor of 5 of each other. The correlation function determined by using the more limited sample agrees well with the correlation function determined for the sample with the simpler selection criteria.

The cross-correlation of Abell clusters with double and multicomponent sources was determined. The correlation amplitude is a factor of ~ 1.6 larger than that obtained for the cross-correlation with the whole sample and ~ 2.5 larger than that obtained for the autocorrelation of this subsample.

4.3. *Flux Cuts and the Presence of Starbursting Galaxies*

We have also analyzed a sample that *excluded* all double and multicomponent sources. Fitting a straight line, one obtains $A = (5.2 \pm 0.4) \times 10^{-3}$ and $\gamma = -0.84 \pm 0.05$ by using the S estimate, and $A = (2.2 \pm 0.4) \times 10^{-3}$ and $\gamma = -1.1 \pm 0.05$ by using the LS estimate. These slopes are shallower than those obtained for the sample as a whole and are more consistent with values determined from optical surveys. The difference is statistically not very significant, but it could be related to the fact that this subsample contains a larger fraction of starbursting galaxies as compared with the sample as a whole. Bright, low-redshift starbusting galaxies are an important component of extragalactic *IRAS* sources that have been shown to have spatial, clustering properties similar to those found for optical galaxies (Davis et al. 1988). The relative contributions of starburst galaxies and active galactic nuclei (AGNs) to the cumulative radio source counts is given in BWH as a function of flux density (based on Windhorst et al. 1985 and Condon 1984). Below 1.0 mJy, the ratio of the number of starbursting galaxies to the number of AGNs (including all giant ellipticals) is approaching unity. Above 3 mJy, this ratio becomes orders of magnitude smaller. To investigate the contribution of starbursting galaxies to the correlation function, the "singles" catalog was divided into catalogs of sources with flux densities below 2 mJy and above 3 mJy, respectively. The results are shown in Figure 4. Best-fit parameters to the $S < 2$ mJy sources are $A = (8.2 \pm 1) \times 10^{-3}$ and $\gamma = -0.84 \pm 0.05$ using the S estimator, and $A = (5.6 \pm 0.6) \times 10^{-3}$ and $\gamma = -0.97 \pm 0.04$ using the LS estimator. A similar result is obtained for a sample with 2 mJy $< S <$ 3 mJy, indicating that incompleteness is not a problem here. The shallow slope and large amplitude are consistent with there being a larger contribution from "nearby" starbursting galaxies with clustering properties more similar to optical galaxies. Best-fit parameters to the $S > 3$ mJy sample are $A = (1.9 \pm 0.4) \times 10^{-3}$ and $\gamma = -1.10 \pm 0.13$ using the S estimator, and $A = (2.6 \pm 0.8) \times 10^{-3}$ and $\gamma = -1.2 \pm 0.1$ using the LS estimator. Above 3 mJy, the slope is more similar to that obtained for all sources, but the amplitude is significantly lower. Assuming that clustering does not decrease with time, the clustering amplitude of a sample must decrease as the average distance to the sources increases. The results are thus consistent with the $S > 3$ mJy sources being dominated by more distant, unresolved FR I and FR II sources. The lower amplitude could also be related to the presence of a large fraction of quasars—although radio-loud quasars are thought to have a large

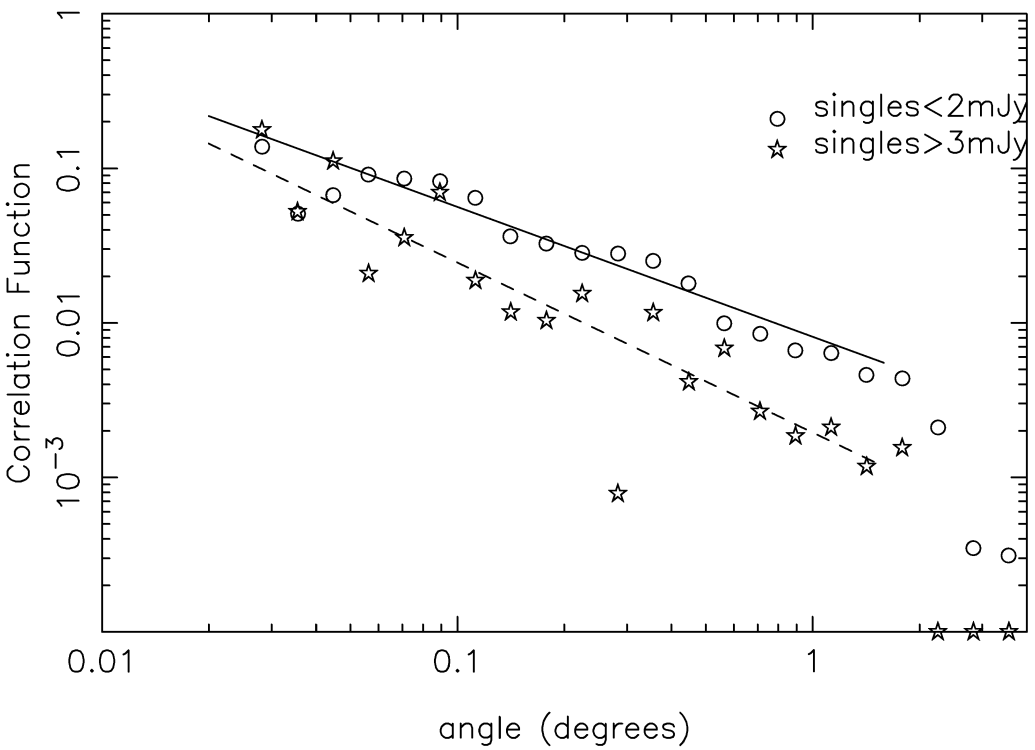

FIG. 4.—The autocorrelation function of two subsamples: the open circles show the results for all single-component sources with flux densities less than 2 mJy, and the stars show the results for single-component sources with flux densities greater than 3 mJy.

clustering amplitude (Bahcall & Chokski 1992), their average distance is larger than that of normal radio galaxies, which will push the clustering amplitude down.

The *whole* sample was also divided into various flux density bins. We determined the correlation function for three samples in which all sources below 2, 3, and 10 mJy were, in turn, excluded. The results were all similar to that determined for the whole survey. This is also true for samples containing sources in 2–10 mJy and 10–35 mJy flux density bins (although the scatter increases as the number of sources decreases). In contrast, all but the deepest of optical surveys display a decrease in the amplitude of the angular correlation as the limiting magnitude is increased (e.g., Maddox et al. 1990). A similar result is not found for radio sources because a lower flux density threshold does not correspond to a deeper survey as it does for optically selected sources. The intrinsic luminosities of radio sources vary over many orders of magnitude, resulting in contributions from sources with a wide range of redshifts, regardless of the flux density threshold. In addition, the appearance of starbursting galaxies decreases the average redshift as thresholds reach 1 mJy. This effect is also seen in the deepest optical surveys. The correlation function for the 1–2 mJy flux cut has a slope ~ 0.85, consistent with a sample containing a significant fraction of starbursting galaxies with clustering properties more similar to optical galaxies.

5. DISCUSSION

Calculations of the correlation function for a preliminary catalog (1994 October) that covered a strip of sky 2°.5 wide in declination and 137° in right ascension appear in Cress et al. (1995). They pointed out that the source extraction algorithms were still being developed and so some changes to the calculation would be inevitable, particularly in the case of multiple sources for which CLEANing is more difficult. An improved version of the catalog covering this 2°.5 wide strip was later made available at the FIRST website (1995 January). Analysis of this improved version showed a significant downward shift in the correlation function. The results for the same strip of sky in the latest catalog (1995 October; the catalog used throughout this work and described in § 2) agree well with the results for the 1995 January catalog. The amplitude of the correlation function for the improved catalogs is 16% lower than that for the catalog used in Cress et al. (1995). The result for the double and multicomponent sources has changed in shape and amplitude.

The power-law fits obtained here agree well with estimates of the angular correlation function for the Green Bank 4.85 GHz survey. That catalog contains 54,579 sources with $0° < \delta < 75°$ and $S > 25$ mJy. About 40% of these were used in the correlation-function analyses by Kooiman et al. (1995) and Sicotte (1995). As a result of the significantly larger number of sources in the FIRST survey, our random errors are, in some cases, as much as a factor of 10 smaller than those estimated from Sicotte's χ^2 contour plots. Our values are within his 30% confidence intervals for the amplitude and slope of the correlation of sources with 35 mJy $< S <$ 900 mJy. The results of Kooiman et al. are also fairly consistent with ours.

Seldner & Peebles (1978) investigated the angular correlation function of radio sources in the 4C catalog, which contains 4836 sources with $-7° < \delta < 80°$ and $S > 2$ Jy. The correlation signal was barely detectable, but they estimated the amplitude of the correlation to be 0.02 at 2°. Assuming $\Omega = 1$, they derived a relation between the angular correlation function of two populations and the spatial correlation via the luminosity functions of those populations. This enabled them to estimate the amplitude of the spatial correlation function of the radio sources (assuming power-law behavior). Their best fit gave a spatial correlation scale of $r_0 \sim 74\ h^{-1}$ Mpc. Writing their equation (27) for the autocorrelation of radio sources and substituting for N, the number of sources per steradian brighter than flux density S, one obtains

$$w(\theta) = \frac{\int_0^\infty x^4\, dx\phi^2 \int_{-\infty}^{+\infty} dy\xi[r, z(x)]}{\{\int_0^\infty x^2\, dx\phi[\log P, z(x)]\}^2}\,, \tag{2}$$

where the coordinate distance is given by

$$x = \frac{2c}{H_0 a_0}\,[1 - (1 + z)^{-0.5}]\,, \tag{3}$$

and the difference in coordinate distance between two sources separated by distance r is given by y. It is assumed that $y \ll x$, that is, that clustering is only appreciable on scales much less than the distance of the sources. The selection function is given by

$$\phi = \int_{\log P_{\min(S)}}^{\log P_{\max}} \rho\ (\log P, z) d(\log P)\,, \tag{4}$$

where ρ is the density of radio sources at redshift z with luminosity between log P and log $P + d(\log P)$ at 1.4 GHz. $P_{\max}$ is given by the maximum luminosity expected [log P(W Hz^{-1} sr^{-1}) ~ 30] for radio sources. $P_{\min}$ is the minimum luminosity required for a source to be seen at redshift z. This is given by

$$P_{\min} = Sa_0^2 x^2 (1 + z)^{1+\alpha}\,, \tag{5}$$

where α is the spectral index of the source.

Dunlop & Peacock (1990, hereafter DP) have estimated the radio luminosity function (RLF) at 2.7 GHz for steep spectrum and flat spectrum sources separately. Condon (1984) has estimated the RLF at 1.4 GHz. Their estimates are derived from source counts at various wavelengths, from redshifts of only the brighest sources ($S > \sim 1$ Jy), and from photometry of some fainter sources. In a first attempt at comparing Peacock & Nicholson's spatial correlation (see § 1) with that inferred from our measurements of the angular correlation, we assume $\xi(r, z) = (r/r_0)^{\gamma-1}(1 + z)^{-3.8}$. The redshift dependence corresponds to linear growth of density perturbations. Following Seldner & Peebles (1978), we can then estimate the value of r_0 by using Condon's RLF or DP's combined steep and flat RLFs, translated to 1.4 GHz.

We calculated r_0 for $\gamma = -0.8$ and $\gamma = -1.1$ using both DP's models and Condon's model. We estimate r_0 to be 10 h^{-1} Mpc, but this result is rather sensitive to the assumed clustering evolution. A detailed analysis of the results will be presented in another paper (Cress & Kamionkowski 1997).

6. CONCLUSIONS

We have shown conclusively that spatial clustering of radio sources can be detected in the angular projection by using the FIRST survey catalog. Specifically, we find that the angular correlation function for all sources above 1 mJy

shows power-law behavior with $\gamma \sim -1.1$ and $A \sim 3 \times 10^{-3}$ out to $\sim 4°$.

Double and multicomponent sources (FR II and FR I sources) show, on scales less than 0°.2, a correlation amplitude that is larger than that obtained for the whole sample by a factor of 2–3. Fits on these small scales, however, do not seem to extrapolate successfully to larger scales.

The correlation function of the faintest sources (<2 mJy) appears to have a slope that is significantly shallower than that for the brighter sources, suggesting a significant contribution from starbursting galaxies at these faint fluxes.

In the future, we will be refining the subsample selection using both source morphology and data on optical counterparts, and we will continue to investigate the derivation of spatial information using luminosity functions and cross-correlations with other populations. This should allow us to probe source clustering to much higher redshifts than has previously been possible.

The success of the FIRST survey is in large measure due to the assistance of a number of organizations. In particular, we acknowledge support from NRAO, NSF (grants AST 94-19906 and AST 94-21178), IGPP/LLNL, the STScI, the National Geographic Society (NGS 5393-094), Columbia University, and Sun Microsystems. This is contribution No. 607 of the Columbia Astrophysics Laboratory.

REFERENCES

Bahcall, N. A., & Chokski, A. 1992, ApJ, 385, L33
Becker, R. H., White, R. L., & Helfand, D. J. 1995, ApJ, 450, 559 (BWH)
Becker, R. H., White, R. L., Helfand, D. J., Gregg, M. D., & McMahon, R. G. 1996, in ASP Conf. Ser. 93, Radio Emission from Stars and the Sun, ed. J. M. Panedes & J. M. Taylor (San Franciso: ASP), in press
Bernstein, G. M. 1994, ApJ, 424, 569
Condon, J. J. 1984, ApJ, 287, 461
Cress, C. M., Helfand, D. J., Becker, R. H., Gregg, M., & White, R. L. 1995, in ASP Conf. Ser. 88, Clusters, Lensing and the Future of the Universe, ed. V. Trimble & A. Reisenegger (San Francisco: ASP), 193
Cress, C. M., & Kamionkowski, M. 1997, MNRAS, submitted
Davis, M., Meiksin, A., Strauss, M. A., Da Costa, L. N., & Yahil, A. 1988, ApJ, 333, L9
Davis, M., & Peebles, P. J. E. 1983, ApJ, 267, 465
Dunlop, J. S., & Peacock, J. A. 1990, MNRAS, 247, 19 (DP)
Fanaroff, B. L., & Riley, J. M. 1974, MNRAS, 167, 31P
Fisher, K. B., Davis, M., Strauss, M. A., Yahil, A., & Huchra, J. 1994, MNRAS, 266, 50
Groth, E. J., & Peebles, P. J. E. 1977, ApJ, 217, 385
Hamilton, A. J. S. 1993, ApJ, 406, L47
Hill, G. J., & Lilly, S. J. 1991, ApJ, 367, 1
Kooiman, B. L., Burns, J. O., & Klypin, A. A. 1995, ApJ, 448, 500
Landy, S. D., & Szalay, A. S. 1993, ApJ, 412, 64 (LS)
Ling, E. N., Frenk, C. S., & Barrow, J. D. 1986, MNRAS, 223, 21P
Maddox, S. J., Efstathiou, G., Sutherland, W. J., & Loveday, J. 1990, MNRAS, 242, 43P
Masson, C. 1979, MNRAS, 188, 261
Peacock, J. A., & Nicholson, D. 1991, MNRAS, 253, 307
Peebles, P. J. 1980, The Large Scale Structure of the Universe (Princeton: Princeton Univ. Press)
Seldner, M., & Peebles, P. J. E. 1978, ApJ, 225, 7
Shaver, P. A., & Pierre, M. 1989, A&A, 220, 35
Sicotte, H. 1995, Ph.D. thesis, Princeton Univ.
Webster, A. 1976, MNRAS, 175, 71
Windhorst, R. A., Miley, G. K., Owen, F. N., Kron, R. G., & Koo, D. C. 1985, ApJ, 289, 494
White, R. L., Becker, R. H., Gregg, M. D., & Helfand, D. J. 1996, ApJ, submitted (WBGH)